

Article

Optimal Operation of a Benchmark Simulation Model for Sewer Networks Using a Qualitative Distributed Model Predictive Control Algorithm

Antonio Cembellín ^{1,*}, Mario Francisco ¹ and Pastora Vega ²¹ Computing and Automation Department, Higher Technical School of Industrial Engineering, University of Salamanca, 37700 Béjar, Spain; mfs@usal.es² Computing and Automation Department, Faculty of Science, University of Salamanca, 37008 Salamanca, Spain; pvega@usal.es

* Correspondence: cembe@usal.es; Tel.: +34-923-4080-800 (ext. 2237)

Abstract: This article presents a distributed model predictive control algorithm including fuzzy negotiation among subsystems and a dynamic setpoint generation method, applied to a simulated sewerage network. The methodology considers WWTP as an additional objective of control. To improve the performance of a DMPC using a hydraulic model for prediction, a more detailed model has been considered including suspended solids concentration (TSS). The results obtained with the proposed methodology have been validated on a benchmark simulation model for sewer systems developed to test and compare methodologies, showing good performance.

Keywords: distributed model predictive control (DMPC); sewer network; fuzzy logic

1. Introduction



Citation: Cembellín, A.; Francisco, M.; Vega, P. Optimal Operation of a Benchmark Simulation Model for Sewer Networks Using a Qualitative Distributed Model Predictive Control Algorithm. *Processes* **2023**, *11*, 1528. <https://doi.org/10.3390/pr11051528>

Academic Editors: Jean-Pierre Corriou and Anthony Rossiter

Received: 27 March 2023

Revised: 27 April 2023

Accepted: 12 May 2023

Published: 17 May 2023



Copyright: © 2023 by the authors. Licensee MDPI, Basel, Switzerland. This article is an open access article distributed under the terms and conditions of the Creative Commons Attribution (CC BY) license (<https://creativecommons.org/licenses/by/4.0/>).

One of the most important resources for humans on earth is water, which becomes easily polluted due to human activities. An adequate wastewater treatment may clean the water to be used again, making this cycle sustainable. Urban drainage systems (UDS) collect and transport both wastewater resulting from human activity and rainfall to treatment facilities avoiding discharges into the environment, forming a combined urban drainage system (CUDS). These systems mainly consist of storage tanks and connecting pipes, constituting a sewer network. After heavy rain events, the wastewater obtained can overflow the network and pollute the environment.

Obtaining mathematical models of the process that enable the design of different control algorithms has been the main research in this field. The operating objectives are essentially to avoid losses of wastewater from the network due to overflows in the storage reservoirs and at the inlet to the WWTP and to maximize this inlet flow, decreasing the economic cost of operation [1,2]. Moreover, reducing the pollutant mass escaping from the network may be a prior objective, so it is needed to consider the concentration of pollutants in the overflowed water [3,4]. Another problem is the “first flush” when abundant precipitation falls after a dry season, provoking a large growth in the concentration of contaminants in the sewer system [5].

Simulation models must accurately describe the processes that occur in a sewerage system (hydraulic and pollutant mass transport). They must be simple enough to be used for control. The features of the wastewater caught depending on the area (urban or industrial wastewaters with variable concentrations of contaminants) and the rainwater going into the network, as well as the specific period of the year, are considered in these models. In consequence, typical patterns that attempt to represent different situations have been developed [6]. Some of them are benchmarks for testing control systems of the sewage, such as [5], and simpler ones can be obtained to be used for advanced control

design algorithms. In general, control strategies for UDS [7] can be off-line controllers, which use static rules, and on-line controllers that use real-time control actions [8–10]. Within the first group, RBC (rule-based control) algorithms have been used in [11,12], with their main problem being the number of rules when the scale of the system grows. Control systems based on fuzzy logic control (FLC), combining simple rules with an expert system, are applied in [13–16]. Within the second group of algorithms, the LQR controller has been used in [17] to reduce the overflows in the network by using all the available storage volume and emptying the system immediately, if possible. Additionally, genetic algorithms have been used in water quality networks in [3] and to optimize the control of UDS [4]. In [12], evolutionary algorithms (EA) together with self-adaptive strategies get an increase in the quality of the water reaching the rivers, reducing costs. Control algorithms based on population dynamics (PD) have been used in [18,19], getting a better use of the sewage capacity and reducing overflows. All the above control strategies are based on sewer network hydraulic models, except in [20,21], in which the concentration of wastewater pollutants is considered in the control algorithm. A literature review of modelling and control of sewer systems is presented in [22].

Related to the structure of the UDS control systems, centralized control is the most used configuration. However, decentralized control using local controllers may be a better solution if the number of actuators is high [23]. In complex large-scale systems, both levels of control (local and global) are usually considered together and frequently, and there can be one more level of control, becoming a hierarchical structure [24,25].

The interaction between the UDS and the WWTP must be considered to improve performance in both systems [26], but there are only few studies in the literature that tackle both systems together and, mainly, they deal with the performance of the WWTP, using simpler models for the sewage systems [27,28]. Considering other control algorithms, in [29] is used a heuristic-type controller based on rules, and in [30], another that combines model predictive control (MPC) with RBC strategies.

One of the most popular advanced control strategies is MPC that uses a system model to obtain the control variables values on a future horizon by optimizing a cost function [31–33]. The MPC algorithm consists of four main parts: a control-oriented prediction model of the process, a cost function representing the control objective, a group of process constraints, and a minimization problem solved in a receding-horizon way [31]. Generally, hierarchical control architectures use the MPC to calculate optimal set-points for local controllers. The features of MPC strategies have several advantages for being used in UDS, such as their ability to predict the system's behavior to future rain events considering delays, constraints, and disturbances. A centralized predictive controller, applied in [25], has been developed considering a model whose state variables are the levels of the network reservoirs, the manipulated variables are flow rates at the tank outputs, and the measurable disturbances are the collected input flow rates to the system. In this case, the main constraints are given by the maximum capacity of tanks and pipes.

In [25,34], an MPC controller has been simulated, obtaining important decreases in floods and overflows. In other cases, MPC algorithms have been applied to UDS by means of non-linear prediction models and both operation costs and overflows have decreased [35,36]. Most parts of the control-oriented models in MPCs consider the hydraulic part only. However, in [20,37], a dynamic model of concentration of suspended solids (TSS) used for the MPC algorithm to minimize not only the CSO volume, but also the total pollutant mass escaping into the environment, is presented. Moreover, in [38], a comparison of two optimization methods to minimize overflows is shown: mixed integer (MI) and quadratic program (QP). This analysis concludes that both methods have the same performance, but QP is computationally more efficient than MI.

In the case of large-scale systems, it can be more suitable to split the whole process into smaller subsystems to simplify the application of MPC controller [9,39]. Then, local prediction models and cost functions are used, and the exchange of information between subsystems may be considered or not. Distributed model predictive control (DMPC) [9]

is applied when local controllers exchange data to solve their own local problem, in a cooperative and coordinated way. In the literature, there is a wide variety of DMPC algorithms applied to different processes [40,41], but only a few deal with water management systems, such as volume control in tanks [42,43] and the coordination of drinking water systems [41,44]. In addition, no applications to sewer systems based on DMPC algorithms considering the concentrations of pollutants have been developed before, to the knowledge of the authors.

Therefore, the major contribution of this article is the development and application of a practical DMPC algorithm to a UDS, using local linearized models of the process including TSS and fuzzy negotiation among the subsystems [42,43]. Moreover, the WWTP is included in the control algorithm as an additional objective which consists of the maximization of the WWTP input flow. The results, obtained from the benchmark described in [5], have been compared with a centralized MPC and DMPC based in a cooperative game [45] to validate the utility of the proposed methodology, providing a comprehensive framework for validation including pollutants and other practical issues.

This document begins with an introduction describing the benchmark simulation model and presenting the model used by the control algorithms. In the next section, its sectorization is detailed. This article follows with the exposition of the control objectives. Then, centralized and distributed MPC control strategies are explained, showing the compared results in each case considering or not considering TSS. Finally, the conclusions of this work are presented.

2. Benchmark Model and Evaluation Criteria

2.1. Benchmark Model Description

The model describes, in a realistic way, the operation of a sewer network, being excellent for testing different control strategies that optimize the performance of the system. This benchmark simulation model for a sewer system [5] has algorithms to produce different scenarios that include both the features and the volume of urban wastewater and the runoff reaching the sewer network, generated by rainfall of variable duration and intensity, considering the season of the year or day of the week. The generation of wastewater at each catchment area combines several contributions: domestic, industry, stormwater, and infiltration to sewage. The pollutants included are chemical oxygen demand (COD), which can be divided into soluble COD and particulate COD; ammonia (NH_4^+); nitrate (NO_3^-); and phosphate (PO_4^{3-}). Particulate COD is the main component of suspended solids. There are six catchment areas (Figure 1), numbered from 1 to 6.

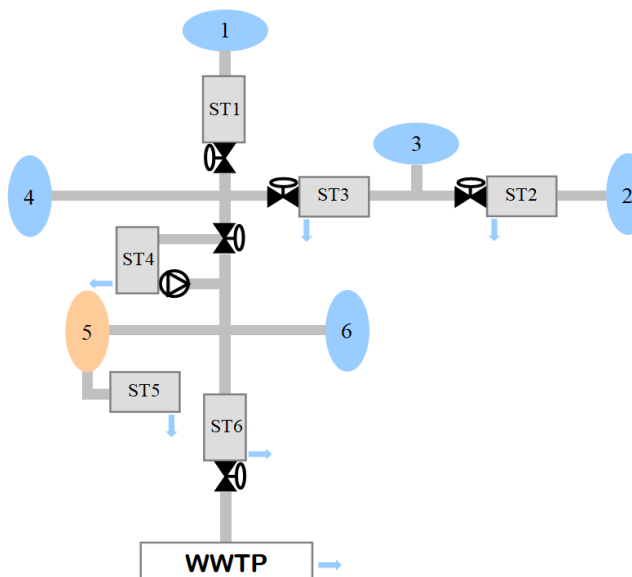


Figure 1. Catchment and sewer network model.

The sewer model consists of three elements: a transport submodel describing the evolution of both flow rate and pollutants in the sewer, a first flush submodel representing the sudden increase of particulates when the rain starts after a long period of drought, and several types of storage tank submodels. This model, shown in Figure 1, is made up of six storage tanks, named ST1, . . . , ST6 (ST5 is an off-line tank); water links; a pump and five valves for flow control; and a wastewater treatment plant.

The major objective of the sewage network is to catch all the urban residual water and lead it to the WWTP, keeping constant a supply flow as close as possible to its nominal inflow rate. This can be obtained by holding the wastewater in the tanks and releasing when the inflow of the WWTP decreases. Moreover, another objective is to minimize the overflows in the deposits and at the inlet of WWTP when rainfall is so intense that it can cause flooding and discharges of contaminant substances into the environment.

As a part of the process of design and assessment of the controllers, a simplified model of the system has been developed and used for the control algorithm. The simplifications consist of considering the hydraulic part of the benchmark together with the concentration of suspended solids TSS, disregarding variables that represent concentrations of other pollutants. The ST5 tank has been eliminated because in this configuration, it is not controllable. The ST6 deposit has been renumbered as 5. In addition, the ST4 reservoir is considered like the rest because the inlet valve is fixed, and the outlet flow is generated by opening a valve instead of activating the pump. In consequence, the mathematical model of the system contains the following parts [5]:

Water catchment areas: zones when the water is collected constituting the inlet flow to the sewage that is considered as a disturbance. The resultant flow in each zone are represented by q_{ri} , $i = 1, \dots, 6$.

Link elements: gravity wastewater pipes in an open channel. They connect the resultant flows in each zone with the deposits, and the deposits with each other and with the WWTP. They are represented as first-order systems with very slow dynamics, depending on their length, including the concentration of total suspended solids, as shown in [37]. Their discrete mathematical model is:

$$\begin{aligned} q_i(k+1) &= \left(1 - \frac{T}{\tau_i}\right)q_i(k) + \left(\frac{T}{\tau_i}\right)q_{u,i}(k), \\ Tss_{out,i}(k+1) &= (1 - c_i)Tss_{out,i}(k) + c_iTss_{in,i}(k), i = 1, 2, 3, \dots, 9, \end{aligned} \quad (1)$$

where:

T is the sampling period;

τ_i is the time constant of the element i ;

$q_i(k)$ is the output flow of the element i ;

$Tss_{out,i}$ is the concentration of suspended solids in the output flow of the element i ;

$q_{u,i}(k)$ is the sum of inflows to the link element i ;

$Tss_{in,i}$ is the concentration of suspended solids in the input flow of the element i ;

c_i is the sedimentation coefficient of suspended in the element i (parameter that needs calibration);

Storage tanks: deposits for storing wastewater. Wastewater stored can overflow if a maximum tank volume is overcome. Their discrete model for the water level and TSS is:

$$\begin{aligned} h_i(k+1) &= h_i(k) + \frac{T}{A_i}[u_{in,i}(k) - u_i(k) - q_{ov,i}(k)] \\ u_i(k) &= a_i(k)c_{0i}\sqrt{h_i(k)}, V_i(k) = A_i h_i(k), V_{max,i} = A_i h_{max,i} \\ Tss_{out,i}(k+1) &= (1 - c_i)Tss_{out,i}(k) + c_i Tss_{in,i}(k), i = 1, 2, 3, 4, 5, \end{aligned} \quad (2)$$

where all parameters are related to tank i and instant k :

$V_{max,i}$ is the maximum capacity of the tank;

$V_i(k)$ is the filled volume;

$Tss_{in,i}$ is the concentration of suspended solids in the input flow of the tank i ;

$Tss_{out,i}$ is the concentration of suspended solids in the output and overflow flow of the tank i ;

$u_{in,i}(k)$ is the input flow rate;
 $u_i(k)$ is the output flow rate;
 $q_{ov,i}(k)$ is the overflow flow rate;
 c_{0i} is the discharge coefficient (experimental parameter depending on the tank i);
 c_i is the sedimentation coefficient of suspended in the tank i (parameter that needs calibration);
 A_i is the tank area;
 $h_{max,i}$ is the tank height;
 $h_i(k)$ is the water level;
 $a_i(k)$ is the opening of the deposit outlet valve (control variable: $a_i \in [0, 1]$);

Nodes: they are places of union of several water pipes. The output flow is the addition of the input flows, and the concentration of suspended solids at the outlet is obtained assuming that the mass of suspended solids is conserved in the node [37]. For example, for a node where three pipes join:

$$\begin{aligned} q_{in3}(k) &= q_{out1}(k) + q_{out2}(k) \\ q_{in3}(k)Tss_{in3}(k) &= q_{out1}(k)Tss_{out1}(k) + q_{out2}(k)Tss_{out2}(k) \\ Tss_{in3}(k) &= \frac{q_{out1}(k)Tss_{out1}(k) + q_{out2}(k)Tss_{out2}(k)}{q_{out1}(k) + q_{out2}(k)}, \end{aligned} \quad (3)$$

In Figure 2, the node model of the example is shown.

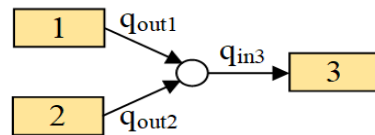


Figure 2. Node model.

Therefore, the expression that allows the calculation of the concentration of solids at the outlet of a node has a non-linear relationship with the flows and concentrations of solids at the inlet of the node, which will also be considered as state variables of the process. As such, to get a linear model of this system, which can be part of the control algorithm, we have to linearize the following expression:

$$\begin{aligned} Tss_{in3} &= \frac{q_{out1}Tss_{out1} + q_{out2}Tss_{out2}}{q_{out1} + q_{out2}} \approx K_{qout1}q_{out1} + K_{qout2}q_{out2} + K_{Tssout1}Tss_{out1} + K_{Tssout2}Tss_{out2}, \\ \text{where : } K_{qout1} &= \frac{q_{out20}(Tss_{out10} - Tss_{out20})}{(q_{out10} + q_{out20})^2}, \quad K_{qout2} = \frac{q_{out10}(Tss_{out20} - Tss_{out10})}{(q_{out10} + q_{out20})^2} \\ K_{Tssout1} &= \frac{q_{out10}}{q_{out10} + q_{out20}}, \quad K_{Tssout2} = \frac{q_{out20}}{q_{out10} + q_{out20}}, \end{aligned} \quad (4)$$

are coefficients calculated for each sampling time at the point of operation from the values of the flow rates and concentrations of solids measured at that point.

The whole system is shown in Figure 3, depicted by a block diagram made of these simple elements: catchments, represented by ovals; storage tanks, by triangles; and link elements, by rectangles. This diagram is like the benchmark represented in Figure 1, but more detailed.

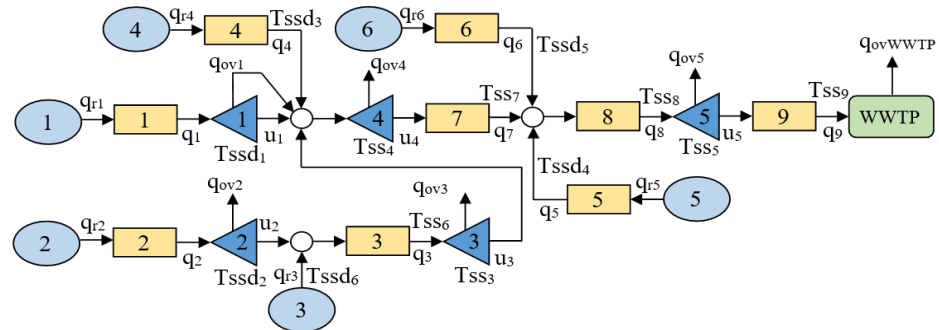


Figure 3. Simplified sewer block diagram.

The state variables are the tank levels 1, 2, 3, 4, and 5 (x_1, \dots, x_5); the flow rates of the pipes 3, 7, 8, and 9, corresponding to the states (x_6, \dots, x_9); and the concentrations of suspended solids in each of them, respectively, except in tanks 1 and 2, since in these cases, the concentrations are not controllable (x_{10}, \dots, x_{16}) because the inlet flow to these tanks cannot be controlled and this is the only way to modify their concentrations. Moreover, the output flow of pipe 9 (state x_9) is the inlet flow to the WWTP if it does not exceed its nominal value. The output flows of the pipes of the catchments 1, 2, 4, 5, and 6, as well as the flow caught in zone 3, will represent measurable disturbances on the system (d_1, \dots, d_6), as well as the concentrations of suspended solids in tanks 1 and 2, in the outlet flows of the link elements of the catchment areas 4, 5, and 6, and in the flow caught in zone 3 (d_7, \dots, d_{12}). The overflowed volume in reservoir 1 returns to the sewer through tank 4. The control variables are the desired output flows of the tanks. They also are the set-points of local PID flow controllers at a lower level (u_1, \dots, u_5). Therefore, the state vector, the control variables vector, and the disturbances vector are defined considering the benchmark variables as:

$$\mathbf{x} = (h_1, h_2, h_3, h_4, h_5, q_3, q_7, q_8, q_9, Tss_3, \dots, Tss_9), \mathbf{u} = (u_1, u_2, u_3, u_4, u_5), \\ \mathbf{d} = (q_1, q_2, q_4, q_5, q_6, q_{r3}, Tssd_1, \dots, Tssd_6), \quad (5)$$

Table 1 shows the system variables and their correspondence with the considered variables of the state space model.

Table 1. System variables.

Space State Model Variables	System Variables	Meaning and Units
x_1, \dots, x_5	h_1, \dots, h_5	Tank levels (m)
x_6, x_7, x_8, x_9	q_3, q_7, q_8, q_9	Pipes 3, 7, 8, and 9 flow rates (m^3/d)
x_{10}, x_{11}, x_{12}	Tss_3, Tss_4, Tss_5	Suspended solids in tanks 3, 4, and 5 (g/m^3)
$x_{13}, x_{14}, x_{15}, x_{16}$	$Tss_6, Tss_7, Tss_8, Tss_9$	Suspended solids in pipes 3, 7, 8, and 9 (g/m^3)
u_1, \dots, u_5	u_1, \dots, u_5	Tank output flow rates (m^3/d)
$d_1, d_2, d_3, d_4, d_5, d_6$	$q_1, q_2, q_4, q_5, q_6, q_{r3}$	Catchment flow rates (m^3/d)
d_7, \dots, d_{12}	$Tssd_1, \dots, Tssd_6$	Catchment suspended solids (g/m^3)

The mathematical model, in terms of discrete differential equations, is:

$$\begin{aligned} x_1(k+1) &= x_1(k) + \frac{T}{A_1}[d_1(k) - u_1(k) - q_{ov1}(k)] \\ x_2(k+1) &= x_2(k) + \frac{T}{A_2}[d_2(k) - u_2(k) - q_{ov2}(k)] \\ x_3(k+1) &= x_3(k) + \frac{T}{A_3}[x_6(k) - u_3(k) - q_{ov3}(k)] \\ x_4(k+1) &= x_4(k) + \frac{T}{A_4}[d_3(k) + u_1(k) + q_{ov1}(k) + u_3(k) - u_4(k) - q_{ov4}(k)] \\ x_5(k+1) &= x_5(k) + \frac{T}{A_5}[x_8(k) - u_5(k) - q_{ov5}(k)] \\ x_6(k+1) &= \left(1 - \frac{T}{\tau_3}\right)x_6(k) + \left(\frac{T}{\tau_3}\right)[d_6(k) + u_2(k)] \\ x_7(k+1) &= \left(1 - \frac{T}{\tau_7}\right)x_7(k) + \left(\frac{T}{\tau_7}\right)u_4(k) \\ x_8(k+1) &= \left(1 - \frac{T}{\tau_8}\right)x_8(k) + \left(\frac{T}{\tau_8}\right)[d_4(k) + d_5(k) + x_7(k)] \\ x_9(k+1) &= \left(1 - \frac{T}{\tau_9}\right)x_9(k) + \left(\frac{T}{\tau_9}\right)u_5(k) \\ x_{10}(k+1) &= (1 - c_3)x_{10}(k) + c_3x_{13}(k) \\ x_{11}(k+1) &= (1 - c_4)x_{11}(k) + c_4 \frac{(u_1(k) + q_{ov1}(k))d_7(k) + d_3(k)d_9(k) + u_3(k)x_{10}(k)}{u_1(k) + q_{ov1}(k) + d_3(k) + u_3(k)} \\ x_{12}(k+1) &= (1 - c_5)x_{12}(k) + c_5x_{15}(k) \\ x_{13}(k+1) &= (1 - c_6)x_{13}(k) + c_6 \frac{u_2(k)d_8(k) + d_6(k)d_{12}(k)}{u_2(k) + d_6(k)} \\ x_{14}(k+1) &= (1 - c_7)x_{14}(k) + c_7u_4(k) \\ x_{15}(k+1) &= (1 - c_8)x_{15}(k) + c_8 \frac{d_5(k)d_{11}(k) + x_7(k)x_{14}(k) + d_4(k)d_{10}(k)}{d_5(k) + x_7(k) + d_4(k)} \\ x_{16}(k+1) &= (1 - c_9)x_{16}(k) + c_9u_5(k), \end{aligned} \quad (6)$$

Then, a linear model is obtained from this model, removing the overflow flow rate terms and linearizing the nonlinear equations in the nodes. This will be used as a prediction model in the MPC strategy:

$$\begin{aligned} x_{11}(k+1) &= (1 - c_4)x_{11}(k) + c_4[K_{4Tss1out}d_7(k) + K_{4Tss3out}x_{10}(k) + \\ &\quad + K_{4u1}u_1(k) + K_{4u3}u_3(k) + K_{4q4}d_3(k) + K_{4Tssd3}d_9(k)] \\ x_{13}(k+1) &= (1 - c_6)x_{13}(k) + c_6[K_{6Tss2out}d_8(k) + K_{6u2}u_2(k) + \\ &\quad + K_{6qr3}d_6(k) + K_{6Tssd6}d_{12}(k)] \\ x_{15}(k+1) &= (1 - c_8)x_{15}(k) + c_8[K_{8q7}x_7(k) + K_{8Tss7out}x_{14}(k) + \\ &\quad + K_{8q5}d_4(k) + K_{8q6}d_5(k) + K_{8Tssd4}d_{10}(k) + K_{8Tssd5}d_{11}(k)] \end{aligned} \quad (7)$$

Hence, the state space model equations are:

$$\begin{aligned} \mathbf{x}(k+1) &= \mathbf{Ax}(k) + \mathbf{B}_p\mathbf{u}(k) + \mathbf{B}_d\mathbf{d}(k) \Rightarrow \mathbf{x}(k+1) = \mathbf{Ax}(k) + \mathbf{B} \begin{bmatrix} \mathbf{u}(k) \\ \mathbf{d}(k) \end{bmatrix}, \\ \text{where : } \mathbf{B} &= [\mathbf{B}_p \quad \mathbf{B}_d], \mathbf{x} = (x_1, x_2, \dots, x_{16}), \mathbf{d} = (d_1, d_2, \dots, d_{12}), \\ \mathbf{u} &= (u_1, u_2, \dots, u_5), \end{aligned} \quad (8)$$

The matrices of the model are shown at the end of this paper in Appendix A.

2.2. Evaluation Criteria

The evaluation of the behavior of the system includes different places of overflow in the sewage and at the input of the WWTP. The evaluation criteria used to analyze the effects of the applied control strategies are shown below. Only hydraulic variables are considered in some of them, whereas others also include magnitudes related to water quality. Some of the indices, such as N_{ov} (number of overflows), T_{ov} (duration of overflow), V_{ov} (overflow volume), G_u (degree of usage of WWTP), and S (smoothness in control law application), corresponding to the first group, are shown in [46]. In this work, the following qualitative indices will be considered, where the subscript i stands for a specific overflow point in the system and n is the total number of points:

1. Total suspended solids mass ($Mss_{ov,i}$) (kg): this is the total mass of suspended solids at a specific overflow place i . Considering simulation time in days (d) T_{sim} , if $q_{ov,i}(t)$ is the overflow (m^3/d) and $Tss_i(t)$ is the total suspended solids concentration (g/m^3), the total suspended solids mass of pollutant overflowed at the point i is:

$$Mss_{ov,i} = 10^{-3} \int_0^{T_{sim}} q_{ov,i}(t) Tss_i(t) dt, \quad (9)$$

and the total mass of suspended solids overflowed in the whole sewer is:

$$Mss_{ov} = \sum_{i=1}^n Mss_{ov,i}, \quad (10)$$

2. Ammonia mass ($NH_{ov,i}$) (kg): this is the total mass of ammonia in wastewater escaping from the sewage at a specific overflow place i . If $NH_i(t)$ is the ammonia concentration, the total ammonia mass overflowed at the point i is:

$$NH_{ov,i} = 10^{-3} \int_0^{T_{sim}} q_{ov,i}(t) NH_i(t) dt, \quad (11)$$

and the total mass of ammonia overflowed in the whole sewer is:

$$NH_{ov} = \sum_{i=1}^n NH_{ov,i}, \quad (12)$$

3. Nitrate mass ($NO_{ov,i}$) (kg): this is the total mass of nitrate in wastewater discharged from a specific overflow place i . If $NO_i(t)$ is the nitrate concentration, the total nitrate mass overflowed at the point i is:

$$NO_{ov,i} = 10^{-3} \int_0^{T_{sim}} q_{ov,i}(t) NO_i(t) dt, \quad (13)$$

and the total mass of nitrate overflowed in the whole sewer is:

$$NO_{ov} = \sum_{i=1}^n NO_{ov,i}, \quad (14)$$

4. Phosphate mass ($PO_{ov,i}$) (kg): this is the total mass of phosphate in wastewater escaping from the sewer network at a certain overflow place i . If $PO_i(t)$ is the phosphate concentration, the total phosphate overflowed at the point i is:

$$PO_{ov,i} = 10^{-3} \int_0^{T_{sim}} q_{ov,i}(t) PO_i(t) dt, \quad (15)$$

and the total mass of phosphate overflowed in the whole sewer is:

$$PO_{ov} = \sum_{i=1}^n PO_{ov,i}, \quad (16)$$

5. Overflow quality index (OQI_i) (kg-pollution units/d): this is an aggregated index representing the total mass of pollutants in wastewater discharged into treated water receivers from a determined overflow place i during a simulation time T_{sim} . It includes all the pollutants with different weights, like those used in BSM2 for WWTP [22]. In this case, OQI_i can be approximated as:

$$OQI_i = \frac{1}{T_{sim}} [w_{Tss} M_{ss,ov,i} + w_{NH} NH_{ov,i} + w_{NO} NO_{ov,i} + w_{PO} PO_{ov,i}], \quad (17)$$

and the total index : $OQI = \sum_{i=1}^n OQI_i,$

with $w_{Tss} = 2$, $w_{NH} = 30$, $w_{NO} = 10$, and $w_{PO} = 100$.

3. Sectorization of the System Model

To apply control methodologies to large-scale systems, it is usually necessary to divide the whole system into smaller subsystems. To find the best way to divide the system into smaller ones, a structural analysis has been carried out, so that the subsystems are controllable, reducing their degree of coupling [47]. The direct graph of the system represents the relationships between the different process variables and helps to obtain the best method to split the entire system into subsystems with minimal coupling, holding their reachability [47]. To achieve this objective, the reachability from the input has been tested from the direct graph of the system obtained by applying the same method as in [46]. This is shown in Appendix B of the document, as well as the system sectorization.

For this benchmark, two subsystems are considered: the first includes tanks 1 to 4, links 1 to 4, and catchment areas 1 to 4; and the second, tank 5, links 5 to 9, and catchment areas 5 and 6. To use the distributed MPC exposed in Section 6, the state space local models of each subsystem are obtained as follows, considering the coupling input u_4 to belong to subsystem 1:

$$\begin{aligned}
\mathbf{x}_1(k+1) &= \mathbf{A}_1 \mathbf{x}_1(k) + \mathbf{B}_{p11} \mathbf{u}_1(k) + \mathbf{B}_{p12} \mathbf{u}_2(k) + \mathbf{B}_{d11} \mathbf{d}_1(k) + \mathbf{B}_{d12} \mathbf{d}_2(k), \\
\mathbf{y}_1(k) &= \mathbf{C}_1 \mathbf{x}_1(k), \text{ where } : \mathbf{x}_1 = (x_1, x_2, x_3, x_4, x_6, x_{10}, x_{11}, x_{13}), \mathbf{u}_1 = (u_1, u_2, u_3, u_4), \\
\mathbf{d}_1 &= (d_1, d_2, d_3, d_6, d_7, d_8, d_9, d_{12}), \\
\mathbf{x}_2(k+1) &= \mathbf{A}_2 \mathbf{x}_2(k) + \mathbf{B}_{p21} \mathbf{u}_1(k) + \mathbf{B}_{p22} \mathbf{u}_2(k) + \mathbf{B}_{d21} \mathbf{d}_1(k) + \mathbf{B}_{d22} \mathbf{d}_2(k), \\
\mathbf{y}_2(k) &= \mathbf{C}_2 \mathbf{x}_2(k), \text{ where } : \mathbf{x}_2 = (x_5, x_7, x_8, x_9, x_{12}, x_{14}, x_{15}, x_{16}), \\
\mathbf{u}_2 &= (u_5), \mathbf{d}_2 = (d_4, d_5, d_{10}, d_{11}),
\end{aligned} \tag{18}$$

Properly choosing the rows and columns of \mathbf{A} and \mathbf{B} from the matrices (8), the matrices \mathbf{A}_1 , \mathbf{B}_{p11} , \mathbf{B}_{p12} , \mathbf{A}_2 , \mathbf{B}_{p21} , and \mathbf{B}_{p22} are obtained. Moreover, due to the system's configuration, \mathbf{B}_{p21} only has non-zero elements in the last column, and \mathbf{B}_{p12} , \mathbf{B}_{d12} , and \mathbf{B}_{d21} are null.

4. Control Objectives

The control objectives considered in this system are to keep the WWTP input flow close to its nominal value, taking advantage of its capacity, to reduce the mass of contaminant escaping from the sewage, avoiding overflows in the deposits and at the input of the WWTP, and to optimize operating costs. To get the exposed goal, the set-points of the outlet flow rates of the deposits (control variables) are obtained to reduce the difference between the nominal flow rate and its current value at the inlet to the WWTP. Moreover, the volume of wastewater is distributed among all the reservoirs in the sewerage according to their capacity, which is obtained by optimizing the difference between the wastewater level of each deposit and a dynamically calculated set-point level to get that objective [48]. The effects of the disturbances (collected flows at the catchment areas) will be reduced by the proportional distribution of the wastewater stored in the reservoirs, minimizing the overflows. The control objectives can be expressed as a cost function that includes the partial goals previously exposed [46,49]:

$$J = \sum_{j=1}^M \sum_{k=0}^N w_j \varphi_j(\mathbf{x}(k), \mathbf{u}(k)) \tag{19}$$

where N is the prediction horizon of the MPC presented in 5 and M is the number of objectives considered, φ_j is a partial goal, and w_j is the weight associated to each partial objective φ_j , with $j = 1, \dots, M$.

The partial objectives included in the control problem considered are shown below:

- Minimization of load overflowed and overflows, and uniform distribution of the stored wastewater and the concentration of total suspended solids:

$$\begin{aligned}
\varphi_1(\mathbf{x}(k)) &= \sum_{i=1}^5 q_{ii}(k) (V_i(k) - v_i V_G(k))^2 + \sum_{j=10}^{12} q_{jj}(k) (Tss_{j-7}(k) - Tss_m(k))^2, \\
v_i &= \frac{V_{i\max}}{\sum_{j=1}^5 V_{j\max}}, \quad V_G(k) = \sum_{j=1}^5 V_j(k), \\
\text{with } q_{ii}(k) &= \begin{cases} f_i & x_i(k) \leq h_{\max i} \\ f_i \left(1 + \alpha_i(x_i(k) - h_{\max i})^2 \frac{Tss_i(k)}{Tss_m(k)}\right) & x_i(k) > h_{\max i} \end{cases} \quad x_i(k) \leq h_{\max i} \\
Tss_m(k) &= \frac{\sum_{j=1}^5 V_j(k) Tss_j(k)}{\sum_{j=1}^5 V_j(k)}
\end{aligned} \tag{20}$$

where V_G is the total filled volume in the sewerage at instant k , v_i is a factor that represents the weight of the deposit capacity i in the total available storage volume in the network,

$Tss_i(k)$ represents the concentration of suspended solids of each tank i at the instant k , and $Tss_m(k)$ is the weighted mean concentration of suspended solids at the instant k . The weight $q_{ii}(k)$ allows for the overflows' penalization, growing quadratically with the associated overflow, and also considers if the pollutant concentration $Tss_i(k)$ is higher or lower than the average $Tss_m(k)$ to penalize more or less the mass of pollutant overflowed. Factors f_i and α_i penalize even more overflows in some deposits. Weights $q_{ii}(k)$ and $q_{jj}(k)$ are tuning parameters included as diagonal elements in the $\mathbf{Q}(k)$ matrix below.

2. Maximum usage and minimum overflow at the WWTP influent:

$$\varphi_2(\mathbf{x}(k)) = (Q_{WWTP}(k) - Q_{WWTP\max})^2 \quad (21)$$

where Q_{WWTP} is the inlet flow to the treatment plant (state x_9) at instant k and $Q_{WWTP\max}$ is its nominal value.

3. Control efforts minimization:

$$\varphi_3(\mathbf{u}(k)) = \sum_{i=1}^5 r_{ii} (u_i(k) - u_{iref}(k))^2 \quad (22)$$

where u_{iref} are the output flows to keep the reference level in a deposit, calculated by Bernoulli's law, as explained in Section 5.2. Weights r_{ii} are tuning parameters included as diagonal elements in the \mathbf{R} matrix below.

The global control system has a hierarchical structure. The level set-points are generated for each variable at the upper level to get the cited control objectives. Thus, the MPC controller solves a constrained optimization problem, obtaining the set-points used by local controllers, optimizing the usage of WWTP and operating costs. Then, local controllers apply the control signals to the system [48,50].

5. Predictive Control Problem with Online Linearization

5.1. Optimization Problem

In this work, the centralized predictive control algorithm considers a linear state-space prediction model, including the influence of disturbances. This model changes every time new values of the process variables are taken, due to the linearization of the expressions in each node, so matrices A and B depend on the sample instant k . The key point is that the optimization of (23) is equivalent to minimize Equation (16), where different objectives are considered, by using specific weights $\mathbf{Q}(k)$ and \mathbf{R} in the MPC problem as explained below, related to weight w_j in (19) and the specific performance indices (20), (21), and (22).

The objective function of the MPC contains both the control errors in the system states and the difference between the control sequence and the flow set-point (hence, it penalizes control energy), considering the control and prediction horizons are equal to N :

$$J(k, \mathbf{U}) = \sum_{i=1}^{N-1} \left[\|\hat{\mathbf{x}}(k+i) - \mathbf{x}_{ref}(k)\|_{\mathbf{Q}(k)}^2 + \|\mathbf{u}(k+i) - \mathbf{u}_{ref}(k)\|_{\mathbf{R}}^2 \right] + \mathbf{x}^T(k+N) \mathbf{P} \mathbf{x}(k+N), \quad (23)$$

where $\mathbf{x}_{ref}(k) = (x_{1ref}, x_{2ref}, \dots, x_{16ref})$ and $\mathbf{u}_{ref}(k) = (u_{1ref}, u_{2ref}, \dots, u_{5ref})$ are the states and inputs set-points, and $\mathbf{U}(k) = [\mathbf{u}(k) \quad \mathbf{u}(k+1) \quad \dots \quad \mathbf{u}(k+N-1)]^T$.

For the MPC algorithm, the optimization problem is:

$$\begin{aligned} \mathbf{U}^*(k) = \underset{\mathbf{U}(k)}{\operatorname{argmin}} J(k), \quad \mathbf{U}^*(k) &= [\mathbf{u}^*(k) \quad \mathbf{u}^*(k+1) \quad \dots \quad \mathbf{u}^*(k+N-1)]^T \text{ subject to :} \\ \hat{\mathbf{x}}(k+i+1) &= \mathbf{A}(k) \hat{\mathbf{x}}(k+i) + \mathbf{B}_p(k) \mathbf{u}(k+i) + \mathbf{B}_d(k) \mathbf{d}(k+i), \quad \mathbf{d}(k+i) = \mathbf{d}(k) \\ \hat{\mathbf{x}}(k) &= \mathbf{x}(k) \\ 0 \leq \hat{x}_j(k+i), \quad i &= 0, \dots, N-1, \quad j = 1, \dots, 5 \\ 0 \leq \hat{x}_j(k+i) &\leq q_{\max j}, \quad i = 0, \dots, N-1, \quad j = 6, \dots, 9 \\ 0 \leq u_j(k+i) &\leq u_{\max j}, \quad i = 0, \dots, N-1, \quad j = 1, \dots, 5, \end{aligned} \quad (24)$$

where $q_{\max j}$ and $u_{\max j}$ are the upper bounds for flow rate in the link elements and the tank outputs, respectively.

For the MPC algorithm, the horizon N , matrices $\mathbf{Q}(k)$ and \mathbf{R} , and a terminal penalty for MPC stability, matrix \mathbf{P} , obtained from the Riccati equation [51], are tuning parameters. A variable diagonal matrix $\mathbf{Q}(k)$ includes all control objectives of 4. When an overflow occurs in a deposit, the associated weight grows to further penalize the difference with the level set-point of this deposit. The elements $q_{11}, \dots, q_{55}, q_{99}, \dots, q_{12,12}$ are the non-zero elements of $\mathbf{Q}(k)$ and are calculated by (20), where f_i and α_i are parameters for tuning MPC. All the rest of the elements are zero because they are related to state variables of pipes and their suspended solids concentrations that do not need to be optimized. To penalize the deviations of the flow set-points in respect to their reference and minimize the operating costs, a diagonal matrix \mathbf{R} is used.

This problem is a quadratic optimization problem (QP) with constraints [31]. The developed algorithm holds the last calculated solution, if the optimization problem is not feasible, to avoid failure of the control system.

5.2. Set-Point Determination

Optimal operation can be achieved by a hierarchical controller that calculates the reservoirs' level set-points to distributing the current volume of wastewater among all the deposits considering their maximum capacity [48]. Therefore, it is necessary to calculate for each one its reference level, considering the total capacity of the system and the volume of that tank at each sampling instant:

$$x_{iref}(k) = \left(\frac{V_G(k)}{A_i} \right) v_i, i = 1, \dots, 5, \quad (25)$$

where $x_{iref}(k)$ is the set-point level for deposit i at instant k . Moreover, the nominal input flow to the WWTP is $x_{0,ref} = 60,000 \text{ m}^3/\text{d}$. The reference values for the states $x_{ref10}, \dots, x_{ref12}$, representing pollutant concentrations, are all taken equal to the average value of the pollutant concentration at the instant considered $Tss_m(k)$. The references for the rest of states are irrelevant because the corresponding weight in \mathbf{Q} matrix is 0.

The flow rate set-points are obtained considering the set-point level for each deposit, according to expression:

$$u_{iref}(k) = c_{0i} \sqrt{x_{iref}(k)}, i = 1, \dots, 5, \quad (26)$$

6. DMPC and Fuzzy Negotiation

6.1. Distributed Model Predictive Control (DMPC) with Fuzzy Negotiation

The DMPC strategy presented in this article is based on [52]. It consists of the optimization of local problems including the future behaviour of the inputs of each subsystem and the neighbour, using local constraints and prediction models. The local MPC problems are analogous to the one presented in Section 5.1, adding neighbouring constraints. Two agents compute each optimization problem. Each agent obtains a control sequence for their subsystem, \mathbf{U}_1^* and \mathbf{U}_2^* , at every sampling period, keeping the neighbour control sequence constant to \mathbf{U}_1^s and \mathbf{U}_2^s , respectively, where \mathbf{U}_1^s and \mathbf{U}_2^s are the previous solutions of optimization problem extended to the current k . Then, another optimization problem is solved by agent 2, providing the control law for the neighbour \mathbf{U}_1^w , keeping their constant, as shown in [46]. Note that agent 1 does not solve any additional optimization problem to provide \mathbf{U}_2^w because \mathbf{U}_2 does not affect subsystem 1 because input u_5 belongs to subsystem 2 only. The fuzzy negotiation provides the final control sequences for subsystem 1, \mathbf{U}_1^f considering the two possible solutions available \mathbf{U}_1^* and \mathbf{U}_1^w , because $\mathbf{U}_2^f = \mathbf{U}_2^*$. To apply the fuzzy negotiation, the average input flow to the WWTP, \bar{q}_{WWTP} , and the TSS mass overflowed on average for all tanks in the prediction horizon \bar{m}_{ssov} are obtained for each of the calculated control sequences. Local prediction models, local solutions, and disturbances are considered for this:

$$\bar{q}_{WWTP}(k) = \frac{1}{N} \sum_{i=1}^N \hat{x}_9(k+i), \bar{m}_{ssov}(k) = \frac{1}{N} \sum_{j=2}^5 \sum_{i=1}^N \hat{q}_{ov,j}(k+i) \cdot \hat{Tss}_j(k+i), \quad (27)$$

6.2. Fuzzy Negotiation

The fuzzification process consists of obtaining fuzzy sets from imprecise knowledge of a system or process. Then, fuzzy values are obtained considering numerical values of a certain property. Defuzzification allows the calculation of numerical values of certain output variables applying a rule set to the inputs and interpreting the membership degrees of the fuzzy sets in a specific decision [53,54]. This method is used in a DMPC algorithm with negotiation between agents to get the best solution to the whole system [46].

Fuzzy sets for \bar{q}_{WWTP} and \bar{m}_{ssov} have been considered with trapezoidal shape and obtained in a heuristic way in order to get the best performance of the entire system (Figure 4). In particular, the fuzzy sets related to \bar{m}_{ssov} are adapted depending on the average concentration of TSS. Table 2 shows fuzzy sets parameters corresponding to (28).

$$\mu_{negligible}(\bar{m}_{ssov}, k) = \begin{cases} 1, & \text{if } \bar{m}_{ssov} < a \\ \frac{b-\bar{m}_{ssov}}{b-a}, & \text{if } a \leq \bar{m}_{ssov} < b \\ 0, & \text{if } \bar{m}_{ssov} \geq b \end{cases} \quad \mu_{noticeable}(\bar{m}_{ssov}, k) = \begin{cases} 0, & \text{if } \bar{m}_{ssov} < a \\ \frac{\bar{m}_{ssov}-a}{b-a}, & \text{if } a \leq \bar{m}_{ssov} < b \\ 1, & \text{if } \bar{m}_{ssov} \geq b \end{cases} \quad (28)$$

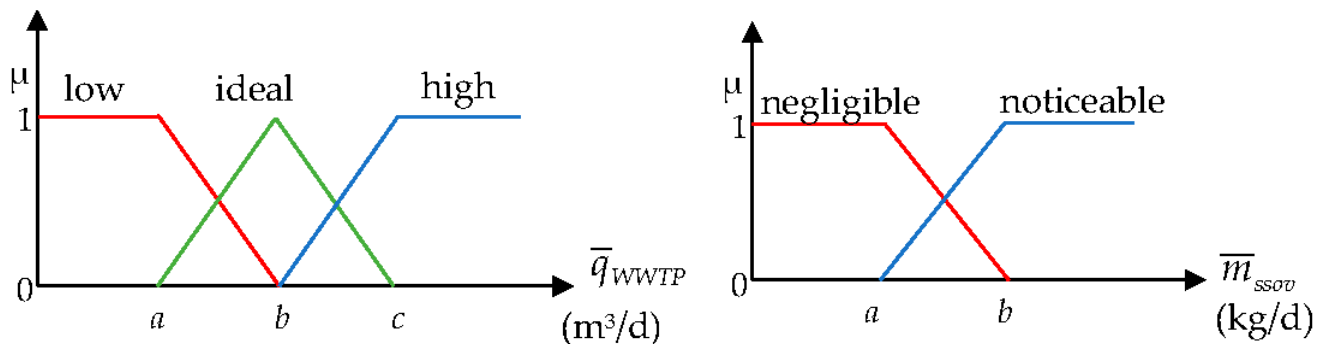


Figure 4. Fuzzy sets for \bar{q}_{WWTP} and \bar{m}_{ssov} .

Table 2. Fuzzy set parameters.

	a	b	c
$\mu(\bar{q}_{WWTP})$	56,000	58,000	60,000
$\mu(\bar{m}_{ssov})$	1000 $Tss_m(k)$	2000 $Tss_m(k)$	-

Fuzzy rules and defuzzification have been carried out following methodology of [46].

7. Results and Discussion

This section presents some simulation results. To reduce the computational time, a period of $Tsim = 10$ days has been taken out from a two-year data series of the benchmark [5], where the flow variability is more significant and represents a specific period of a humid season with heavy rainfall (Figure 5) with their concentrations of suspended solids (Figure 6) and ammonia (Figure 7) as representative pollutants.

To assess the methodology presented in the article, four cases have been considered. The first case (CASE 1, without control) consists of keeping all the tank output valves fully open. The second case (CASE 2, DMPC based on a cooperative game) considers two local MPCs in relation to the models shown in (15) and a negotiation based on a cooperative game shown in [45]. The third case (CASE 3, DMPC with fuzzy negotiation) corresponds to the methodology exposed in this work, and centralized MPC is CASE 4.

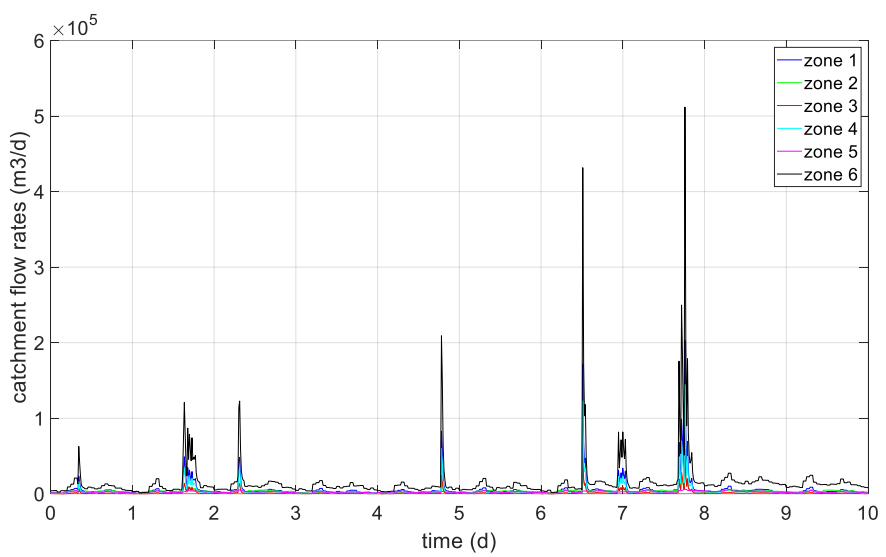


Figure 5. Catchment flow rates.

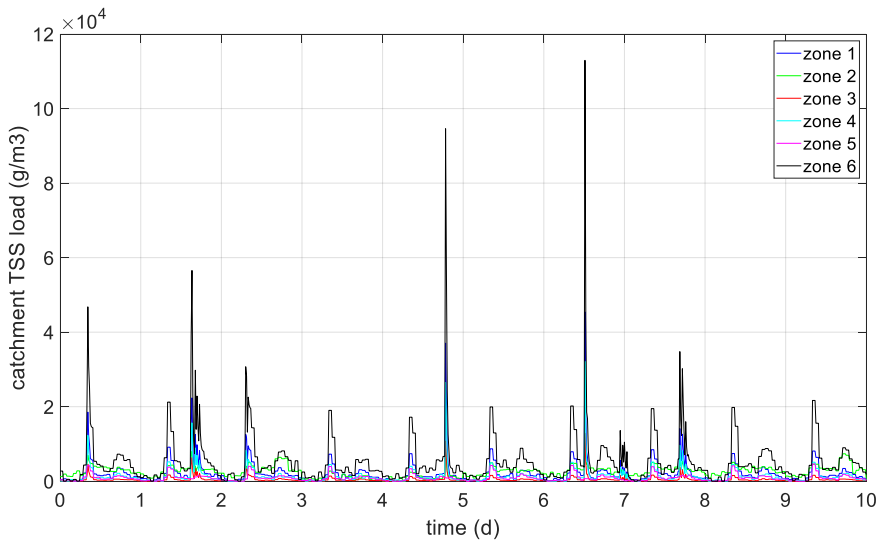


Figure 6. Catchment TSS load.

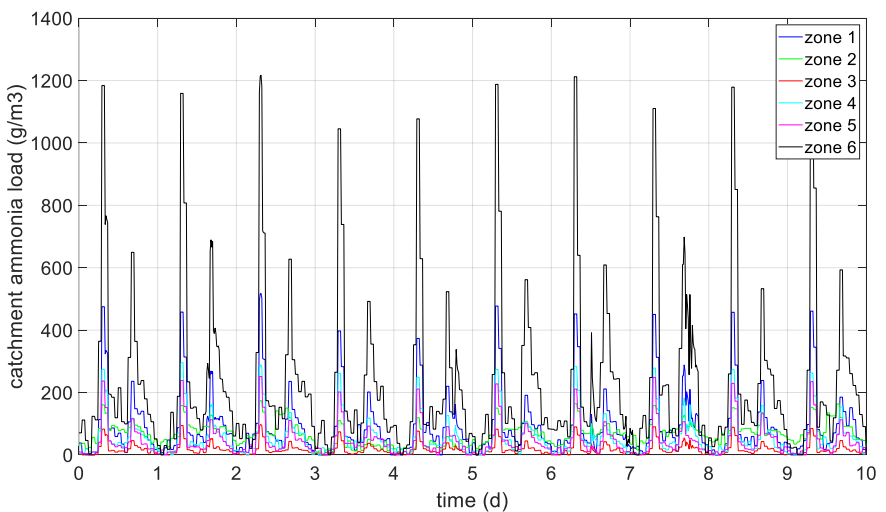


Figure 7. Catchment ammonia load.

In addition, for each control algorithm, two options have been considered depending on whether concentrations of TSS are included or not. The collected water comes from the urban wastewater and intensity variable rainfall events in relation to the season, which are the ones that usually cause the overflow in the deposits and at the input of the WWTP. For all cases, the prediction horizon selected is $N = 5$, and the weights in the cost function are shown in Table 3.

Table 3. Algorithm tuning parameters.

Weights for (19)	Weights for (20), (21)	Weights for (22)
$w_i = 1, i = 1, 2, 3$	$f_i = 10, i = 1, 2, 3, 4, 5$ $\alpha_i = 0, i = 1$ $\alpha_i = 10, i = 2, 3, 4, 5$ $q_{99} = 10^{-5}$ $q_{ii} = 10^{-12}, i = 10, 11, 12$	$r_{ii} = 10^{-8}, i = 1, \dots, 5$

The system parameters are shown in Table 4 (extracted from [5]).

Table 4. System parameters.

Parameter	Units	Values
A_1, \dots, A_5 tank areas	m^2	1188, 252, 348, 852, 2988
c_{01}, \dots, c_{05} discharge coefficients	$\text{m}^{5/2}/\text{d}$	1.89, 0.40, 0.55, 1.36, 6.12 ($\times 10^4$)
$h_{\max 1}, \dots, h_{\max 5}$ tank heights	m	5 (for all)
$h_{\min 1}, \dots, h_{\min 5}$ minimum levels	m	0 (for all)
$q_{\max 1}, \dots, q_{\max 9}$ maximum flow rates at the pipes outlet	m^3/d	5.99, 1.27, 3.02, 4.29, 4.29, 15.06, 4.29, 23.64, 6 ($\times 10^4$)
T sampling time	d	0.0021
τ_1, \dots, τ_9 link elements time constants	d	0.0313, 0.0104, 0.0104, 0.0208, 0.0208, 0.073, 0.0208, 0.0104, 0.0104
$u_{\max 1}, \dots, u_{\max 5}$ maximum flow rates at the reservoirs outlet	m^3/d	5.98, 1.27, 1.75, 4.29, 19.34 ($\times 10^4$)
c_1, \dots, c_9 sedimentation coefficients in tanks and links	-	0.25 (for all)

Firstly, results without including the concentration of TSS are shown as a basis for comparison with the methodology proposed in this paper. In summary, they correspond to the methodology of [46] adapted to be applied to the sewer benchmark [5]. As you can appreciate in Figure 8, the inflow to WWTP has no significant difference for all cases (a), the same for the overflow flow rate (b) at the entrance of WWTP, corresponding with inlet flows higher than its nominal value ($60,000 \text{ m}^3/\text{d}$), except for case 1. The differences between all the cases can be better appreciated in the numerical results of Table 5.

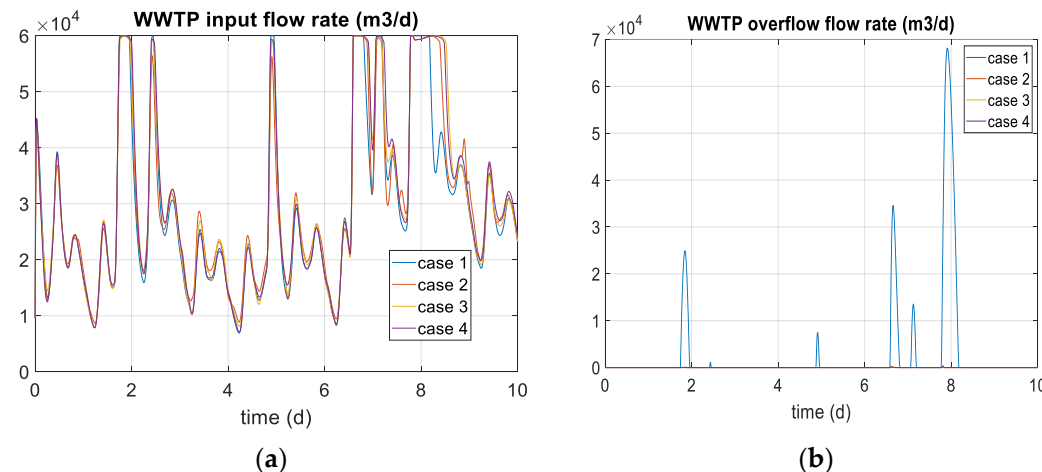


Figure 8. WWTP input (a) and overflow flow rates (b).

Due to the water collected in the catchments having great variability, it is not easy to hold the nominal flow value at the WWTP inlet, and most of the time, it cannot reach this value. However, when any control is applied, more wastewater is retained in deposit 5, producing a better regulation of the WWTP inlet flow (Figure 8a), which is particularly noticeable at the last rainfall peak.

Figure 9 describes the dynamics of some contaminants in the WWTP provided by the benchmark that includes transport models for all pollutants (TSS and ammonia) in each case. No significant differences are observed, but, in general, it is observed that both the peaks and the valleys are more pronounced in the uncontrolled case than in the controlled cases.

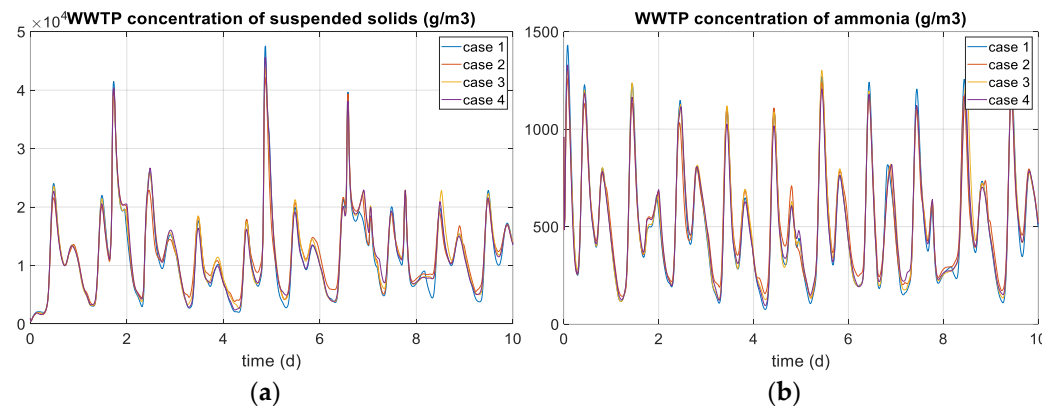


Figure 9. Concentration of suspended solids (a) and ammonia (b) in WWTP input flow rate.

As an example, Figure 10 shows deposit 5 level (a) and outflow set-point (b), u_5 , in each case. The water level signal in tank 5 is shown together with the set-point calculated by the upper level of the hierarchical control system. The set-point tracking is appreciably better for cases 2, 3, and 4 than for case 1, especially at rainfall peaks. Hence, if no control is applied, most overflows are generated at the WWTP inlet because not enough water is being retained in the sewage deposits. Moreover, the controlled cases reduce the total amount of overflows at the WWTP inlet and the total overflowed water volume (Table 4).

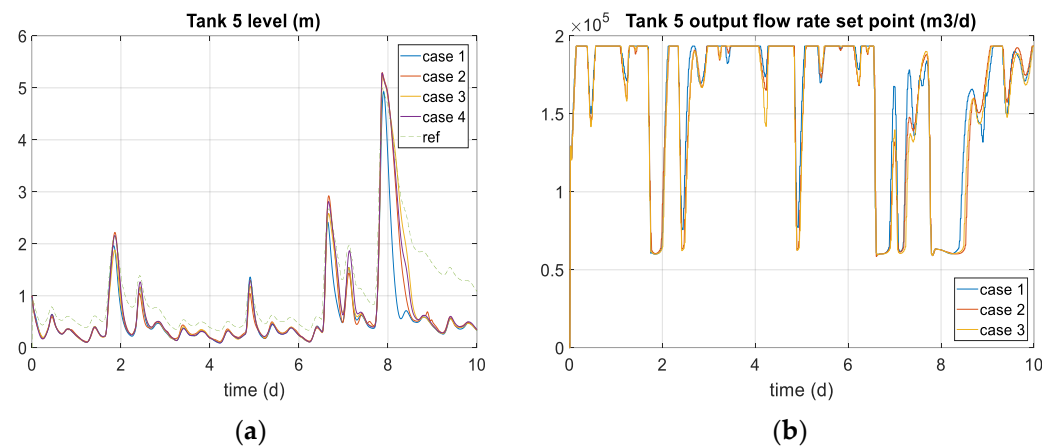


Figure 10. Deposit 5 level (a) and output flow rate reference (b).

The results obtained applying the methodology proposed in this work including TSS are shown in Figures 11–13. There are no significant differences comparing with previous results. Therefore, more insight is obtained from Tables 6 and 7.

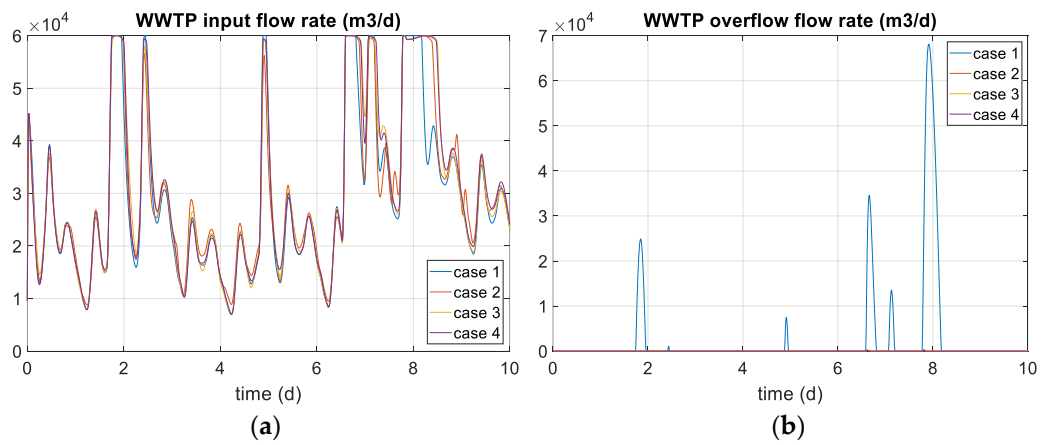


Figure 11. WWTP input (a) and overflow flow rates (b).

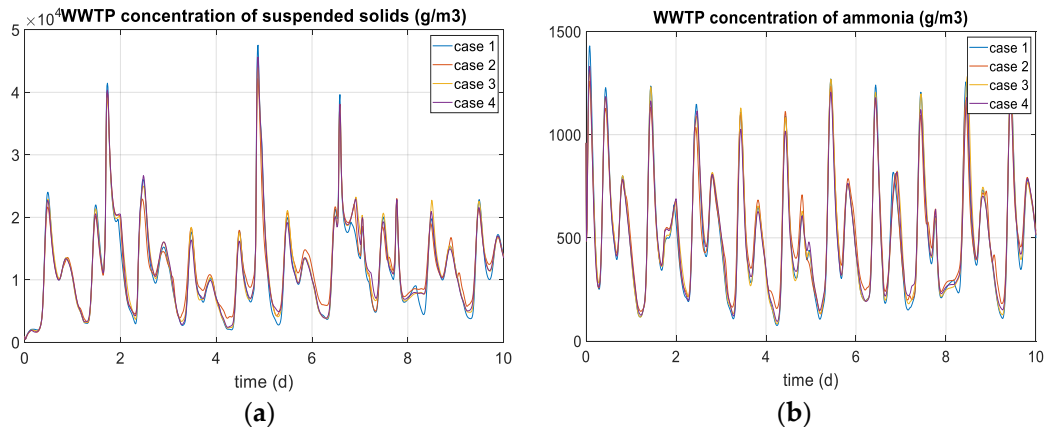


Figure 12. WWTP concentration of suspended solids (a) and ammonia (b).

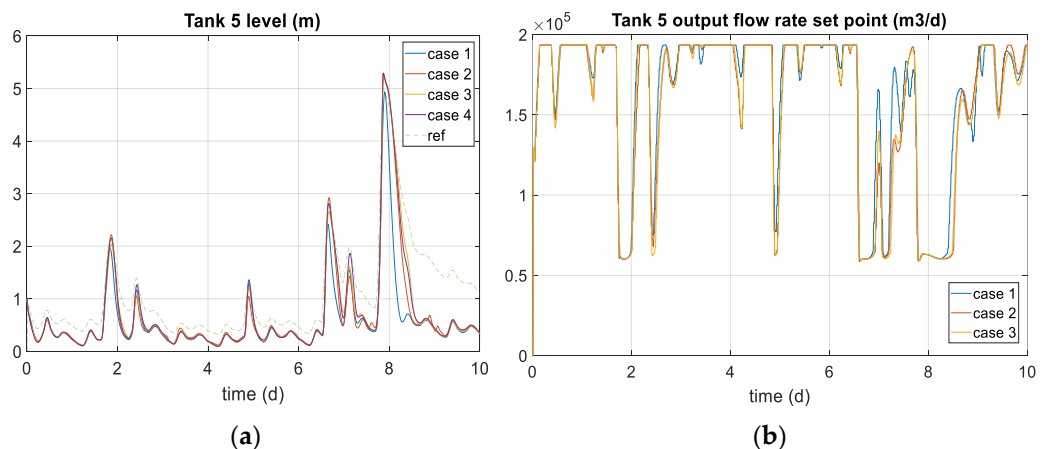


Figure 13. Deposit 5 level (a) and output flow rate set-point (b).

For the four cases, Tables 5 and 6 show the performance indices of Section 2.2. Case 1 (without control) presents the poorest indices, as we expected, and the centralized MPC shows the best behaviour for the average flow at the input WWTP (Q_{WWTP}) for the degree of usage of the treatment plant (G_u), for the total overflowed volume (V_{ov}), and for the total overflowed pollutants (Mss_{ov} , NH_{ov} , NO_{ov} , PO_{ov}). Moreover, the DMPC with fuzzy negotiation does not present a great worsening of those indices, with the advantage of using local optimization problems. Moreover, the smoothing effect of the fuzzy sets selected for negotiation is the reason why the use of fuzzy DMPC obtains the smallest S . The case of DMPC based on a cooperative game provides the worst performance indices of controlled

cases because the negotiation is performed in a discrete way from evaluating costs for different combinations of control actions.

Table 5. Numerical results for controllers without Tss.

Data	No Control	DMPC with Cooperative Game	DMPC with Fuzzy Negotiation	Centralized MPC
$V_{ov,2}$	184.9266	312.9585	292.3083	202.1544
$V_{ov,3}$	644.9788	996.5150	795.6183	681.0547
$V_{ov,4}$	1.8077×10^3	6689.1	7968.8	3130.0
$V_{ov,5}$	0	6577.5	4338.3	5780.0
$V_{ov,WWTP}$	2.6362×10^4	18.0810	20.3194	18.0087
V_{ov}	28,999	14,594	13,415	9811.2
$Mss_{ov,2}$	49.310	96.488	83.922	54.588
$Mss_{ov,3}$	128.37	274.86	192.95	139.19
$Mss_{ov,4}$	207.37	992.50	1131.2	443.44
$Mss_{ov,5}$	0	841.16	519.96	712.53
$Mss_{ov,WWTP}$	5451.6	6.1879	7.0636	5.9378
Mss_{ov}	5836.6	2211.2	1935.1	1355.7
$NH_{ov,2}$	1.2605	2.4402	2.1236	1.3998
$NH_{ov,3}$	3.2733	7.1891	4.9912	3.5657
$NH_{ov,4}$	6.6447	33.5894	35.7513	14.9230
$NH_{ov,5}$	0	27.0282	16.4251	22.6801
$NH_{ov,WWTP}$	126.8435	0.1085	0.1033	0.1024
NH_{ov}	138.0221	70.3554	59.3945	42.6710
$NO_{ov,2}$	0	0	0	0
$NO_{ov,3}$	0	0	0	0
$NO_{ov,4}$	0.0291	0.2452	0.4307	0.1101
$NO_{ov,5}$	0	0.0991	0.0495	0.0772
$NO_{ov,WWTP}$	0.3251	0.0013	6.3448×10^{-4}	6.1315×10^{-4}
NO_{ov}	0.3542	0.3456	0.4808	0.1879
$PO_{ov,2}$	0.1136	0.2168	0.1916	0.1254
$PO_{ov,3}$	0.3818	0.7977	0.5628	0.4135
$PO_{ov,4}$	1.2249	7.3240	6.7831	3.1694
$PO_{ov,5}$	0	5.7923	3.4800	4.8845
$PO_{ov,WWTP}$	26.8422	0.0242	0.0230	0.0227
PO_{ov}	28.5626	14.1550	11.0405	8.6155
OQI_2	23.6549	36.6397	33.1744	25.1296
OQI_3	45.5329	86.6197	63.6188	48.5771
OQI_4	71.5591	310.2451	344.5962	143.8839
OQI_5	10	259.9951	163.6654	221.1111
OQI_{WWTP}	1483.9	11.5668	11.7255	11.4979
OQI	1634.6	705.0665	616.7803	450.1995
Q_{WWTP}	28,860	30,021	30,384	30,556
G_u	48.1006	50.0351	50.6408	50.9265
S	-	1.7334×10^{11}	6.9231×10^{10}	7.6086×10^{10}

The overflow volume in deposit 1 comes back to the sewage due to the system structure. Hence, no parameter is considered.

Table 6. Numerical results for TSS-included option.

Data	No Control	DMPC with Cooperative Game	DMPC with Fuzzy Negotiation	Centralized MPC
$V_{ov,2}$	184.9266	313.2993	201.0480	203.8316
$V_{ov,3}$	644.9788	992.7195	672.6625	666.7686
$V_{ov,4}$	1.8077×10^3	6694.7	7765.2	3123.6
$V_{ov,5}$	0	6682.0	4110.8	5789.3
$V_{ov,WWTP}$	2.6362×10^4	19.1941	24.4878	17.9733
V_{ov}	28,999	14,702	12,774	9801.5

Table 6. Cont.

Data	No Control	DMPC with Cooperative Game	DMPC with Fuzzy Negotiation	Centralized MPC
$Mss_{ov,2}$	49.310	97.191	54.191	55.108
$Mss_{ov,3}$	128.37	275.65	143.04	136.24
$Mss_{ov,4}$	207.37	993.03	1078.7	444.60
$Mss_{ov,5}$	0	857.42	478.05	713.47
$Mss_{ov,WWTP}$	5451.6	6.5113	8.3917	5.9371
Mss_{ov}	5836.6	2229.8	1762.4	1355.3
$NH_{ov,2}$	1.2605	2.4591	1.3826	1.4142
$NH_{ov,3}$	3.2733	7.2185	3.6652	3.4848
$NH_{ov,4}$	6.6447	33.4184	34.3609	14.9650
$NH_{ov,5}$	0	27.4838	15.1051	22.7104
$NH_{ov,WWTP}$	126.8435	0.1183	0.1334	0.1016
NH_{ov}	138.0221	70.6981	59.6472	42.6760
$NO_{ov,2}$	0	0	0	0
$NO_{ov,3}$	0	0	0	0
$NO_{ov,4}$	0.0291	0.2409	0.4353	0.1041
$NO_{ov,5}$	0	0.0998	0.0507	0.0738
$NO_{ov,WWTP}$	0.3251	0.0013	8.8362×10^{-4}	5.7748×10^{-4}
NO_{ov}	0.3542	0.3421	0.4869	0.1784
$PO_{ov,2}$	0.1136	0.2182	0.1249	0.1265
$PO_{ov,3}$	0.3818	0.8010	0.4223	0.4045
$PO_{ov,4}$	1.2249	7.2788	6.2459	3.1790
$PO_{ov,5}$	0	5.8853	3.1999	4.8879
$PO_{ov,WWTP}$	26.8422	0.0263	0.0296	0.0225
PO_{ov}	28.5626	14.2096	10.0227	8.6205
OQI_2	23.6549	36.8371	24.9986	25.2768
OQI_3	45.5329	86.8660	49.6458	47.7420
OQI_4	71.5591	309.8305	329.8800	144.2374
OQI_5	10	264.6245	151.2962	221.3869
OQI_{WWTP}	1483.9	11.6611	12.0823	11.4949
OQI	1634.6	709.8192	567.9028	450.1381
Q_{WWTP}	28,860	30,003	30,430	30,555
G_u	48.1006	50.0050	50.7169	50.9255
S	-	1.7073×10^{11}	6.9069×10^{10}	7.6321×10^{10}

Table 7. Comparative improvement for controllers including TSS.

Data	Included TSS Option	DMPC with Cooperative Game	DMPC with Fuzzy Negotiation	Centralized MPC
V_{ov}	No	14,594	13,415	9811.2
V_{ov}	Yes	14,702	12,774	9801.5
Mss_{ov}	No	2211.2	1935.1	1355.7
Mss_{ov}	Yes	2229.8	1762.4	1355.3
NH_{ov}	No	70.3554	59.3945	42.6710
NH_{ov}	Yes	70.6981	59.6472	42.6760
NO_{ov}	No	0.3456	0.4808	0.1879
NO_{ov}	Yes	0.3421	0.4869	0.1784
PO_{ov}	No	14.1550	11.0405	8.6155
PO_{ov}	Yes	14.2096	10.0227	8.6205
OQI	No	705.0665	616.7803	450.1995
OQI	Yes	709.8192	567.9028	450.1381
Q_{WWTP}	No	30,021	30,384	30,556
Q_{WWTP}	Yes	30,003	30,430	30,555
G_u	No	50.0351	50.6408	50.9265
G_u	Yes	50.0050	50.7169	50.9255

Regarding the numerical results, the performance improves when the concentration of pollutant is considered, except in case 2, although this is not very significant.

However, the best performance improvement is in case 3 because the negotiation between agents considers the overflowed TSS mass. Table 7 shows the comparative performance improvement in each case.

In the end, to analyze how the location of the fuzzy sets affects the behavior of the DMPC algorithm, fuzzy sets have been moved, as shown in Table 8, while preserving their shape.

Table 8. Fuzzy sets parameters for each DMPC case.

Case	$\mu(\bar{q}_{WWTP})$			$\mu(\bar{m}_{ssov})$	
	a	b	c	a	b
DMPC 1	56,000	58,000	60,000	1000 $Tss_m(k)$	2000 $Tss_m(k)$
DMPC 2	54,000	56,000	58,000	1000 $Tss_m(k)$	2000 $Tss_m(k)$
DMPC 3	58,000	60,000	62,000	1000 $Tss_m(k)$	2000 $Tss_m(k)$
DMPC 4	56,000	58,000	60,000	0000 $Tss_m(k)$	1000 $Tss_m(k)$
DMPC 5	56,000	58,000	60,000	2000 $Tss_m(k)$	3000 $Tss_m(k)$

The results not including the concentration of suspended solids (without TSS) are presented in Table 9, and the results including TSS are presented in Table 10.

For the first situation, the DMPC1 and DMPC2 cases show similar results, so the influence of the place of the fuzzy sets is very small. Regarding DMPC3 and DMPC2, the degree of usage of the treatment plant is slightly smaller in DMPC3 because the fuzzy set has been moved to the inlet flow constraint of 60,000 m³/d. By comparing DMPC4 and DMPC3, the overflow (V_{ov}) is larger for DMPC3 because the fuzzy set does not consider minor overflows. In conclusion, the results have no significant differences because the fuzzy sets are very close to each other, but DMPC4 presents the best performance.

Table 9. Numerical results moving DMPC fuzzy sets (without including TSS).

Data	DMPC1	DMPC2	DMPC3	DMPC4	DMPC5
$V_{ov,2}$	292.3083	294.4305	310.7161	261.1050	296.7159
$V_{ov,3}$	795.6183	807.0578	971.8244	687.2200	835.2211
$V_{ov,4}$	7968.8	7974.8	7721.3	7905.4	7820.3
$V_{ov,5}$	4338.3	4341.4	4338.3	4338.3	4343.8
$V_{ov,WWTP}$	20.3194	20.1841	21.2225	20.6859	20.1757
V_{ov}	13,415	13,438	13,982	13,189	13,316
$Mss_{ov,2}$	83.922	84.702	93.652	72.960	85.670
$Mss_{ov,3}$	192.95	196.94	259.77	155.33	206.23
$Mss_{ov,4}$	1131.2	1133.0	1161.4	1129.1	1102.1
$Mss_{ov,5}$	519.96	520.58	613.08	513.98	521.12
$Mss_{ov,WWTP}$	7.0636	7.0119	6.9094	7.2022	6.9319
Mss_{ov}	1935.1	1942.2	2134.8	1878.5	1922.0
$NH_{ov,2}$	2.1236	2.1431	2.3672	1.8504	2.1673
$NH_{ov,3}$	4.9912	5.0960	6.7716	4.0041	5.3391
$NH_{ov,4}$	35.7513	35.7867	39.8640	36.1368	34.5933
$NH_{ov,5}$	16.4251	16.4406	19.8800	16.2649	16.4578
$NH_{ov,WWTP}$	0.1033	0.1027	0.1165	0.1056	0.1034
NH_{ov}	59.3945	59.5692	68.9993	58.3617	58.6610
$NO_{ov,2}$	0	0	0	0	0
$NO_{ov,3}$	0	0	0	0	0
$NO_{ov,4}$	0.4307	0.4410	0.3890	0.4154	0.4276
$NO_{ov,5}$	0.0495	0.0505	0.0643	0.0499	0.0500
$NO_{ov,WWTP}$	6.3448×10^{-4}	6.3597×10^{-4}	8.1386×10^{-4}	6.5225×10^{-4}	6.2756×10^{-4}
NO_{ov}	0.4808	0.4921	0.4541	0.4660	0.4782
$PO_{ov,2}$	0.1916	0.1933	0.2114	0.1675	0.1953
$PO_{ov,3}$	0.5628	0.5744	0.7573	0.4548	0.6013
$PO_{ov,4}$	6.7831	6.7948	8.5241	6.8598	6.5964
$PO_{ov,5}$	3.4800	3.4835	4.2674	3.4520	3.4862
$PO_{ov,WWTP}$	0.0230	0.0228	0.0260	0.0235	0.0230
PO_{ov}	11.0405	11.0687	13.7862	10.9576	10.9022

Table 9. Cont.

Data	DMPC1	DMPC2	DMPC3	DMPC4	DMPC5
OQI_2	33.1744	33.3891	35.8530	30.1599	33.6553
OQI_3	63.6188	64.7335	82.3436	53.1236	67.3239
OQI_4	344.5962	345.0823	363.1114	345.3249	335.2797
OQI_5	163.6654	163.8365	192.7466	161.9850	163.9967
OQI_{WWTP}	11.7255	11.7134	11.7349	11.7601	11.6996
OQI	616.7803	618.7548	685.7893	602.3535	611.9552
Q_{WWTP}	30,384	30,381	30,317	30,401	30,399
G_u	50.6408	50.6354	50.5288	50.6678	50.6643
S	6.9231×10^{10}	6.9375×10^{10}	9.6167×10^{10}	6.9317×10^{10}	6.9414×10^{10}

For the second case, the place of the fuzzy sets affects more than before. This influence is more difficult to establish since the fuzzy sets depend at each instant on the concentration of suspended solids. However, the results have no great differences due to the fuzzy sets being very close to each other, but DMPC3 presents the best performance.

Table 10. Numerical results moving DMPC fuzzy sets (including TSS).

Data	DMPC1	DMPC2	DMPC3	DMPC4	DMPC5
$V_{ov,2}$	203.5121	204.8541	288.4027	204.9085	205.5031
$V_{ov,3}$	672.5447	675.6874	722.9298	673.0609	674.1634
$V_{ov,4}$	7770.5	7701.0	6205.4	7811.8	7880.9
$V_{ov,5}$	4109.7	4142.8	4873.0	4108.9	4113.2
$V_{ov,WWTP}$	24.4633	24.5810	23.1997	24.4242	24.3320
V_{ov}	12,781	12,749	12,113	12,823	12,898
$Mss_{ov,2}$	54.9411	55.2451	82.6870	55.3666	55.5478
$Mss_{ov,3}$	142.9723	143.8091	170.0461	143.3309	144.106
$Mss_{ov,4}$	1079.5	1073.9	880.6759	1083.5	1090.4
$Mss_{ov,5}$	477.9512	482.4708	588.7328	477.9763	478.7065
$Mss_{ov,WWTP}$	8.3843	8.5278	7.6018	8.3672	8.3379
Mss_{ov}	1763.7	1763.9	1729.7	1768.5	1777.1
$NH_{ov,2}$	1.4013	1.4093	2.0927	1.4119	1.4165
$NH_{ov,3}$	3.6634	3.6850	4.3927	3.6732	3.6952
$NH_{ov,4}$	34.3839	34.2258	28.7100	34.5066	34.6885
$NH_{ov,5}$	15.1017	15.2228	18.9341	15.1034	15.1237
$NH_{ov,WWTP}$	0.1332	0.1324	0.1287	0.1330	0.1323
NH_{ov}	54.6835	54.6752	54.2582	54.8281	55.0561
$NO_{ov,2}$	0	0	0	0	0
$NO_{ov,3}$	0	0	0	0	0
$NO_{ov,4}$	0.4302	0.4229	0.3456	0.4393	0.4273
$NO_{ov,5}$	0.0501	0.0502	0.0642	0.0507	0.0487
$NO_{ov,WWTP}$	8.7218×10^{-4}	8.4314×10^{-4}	8.8063×10^{-4}	8.8474×10^{-4}	8.4302×10^{-4}
NO_{ov}	0.4812	0.4739	0.4108	0.4909	0.4768
$PO_{ov,2}$	0.1267	0.1274	0.1889	0.1276	0.1280
$PO_{ov,3}$	0.4221	0.4246	0.4967	0.4231	0.4252
$PO_{ov,4}$	6.2459	6.2178	5.7592	6.2710	6.2872
$PO_{ov,5}$	3.1989	3.2246	4.0418	3.1996	3.2018
$PO_{ov,WWTP}$	0.0296	0.0295	0.0290	0.0296	0.0294
PO_{ov}	10.0232	10.0238	10.5156	10.0509	10.0717
OQI_2	25.2049	25.2895	32.8343	25.3219	25.3717
OQI_3	49.6267	49.8594	57.2369	49.7280	49.9564
OQI_4	330.1006	328.4947	273.1868	331.2860	333.1983
OQI_5	151.2654	152.5351	185.0174	151.2762	151.4811
OQI_{WWTP}	12.0802	12.1066	11.9102	12.0762	12.0682
OQI	568.2778	568.2853	560.1855	569.6883	572.0757
Q_{WWTP}	30,430	30,436	30,474	30,428	30,423
G_u	50.7161	50.7267	50.7896	50.7131	50.7055
S	6.9493×10^{10}	6.8258×10^{10}	8.5400×10^{10}	6.9441×10^{10}	6.9763×10^{10}

8. Conclusions

This work presents a DMPC with fuzzy negotiation applied to a simulated sewage network benchmark, offering good results in comparison with centralized MPC and DMPC based on a cooperative game. Naturally, centralized MPC obtains the best results, as this controller uses the entire model of the system. Nevertheless, the DMPC results have no great differences, but in this case, the control system manages simpler optimization problems and, like other distributed strategies, provides the system with a certain fault tolerance. In comparison with a DMPC based on a cooperative game, fuzzy negotiation improves the results significantly. In addition, the fuzzy negotiation includes expert knowledge of the sewer system considering fuzzy sets whose shape is real-time adapted to the process depending on the needs of the sewer system.

Moreover, only DMPC with a fuzzy negotiation algorithm considering the concentration of suspended solids improves the performance of the sewer system even more, reducing both the volume and the pollutant mass overflowed in the whole of the system, whereas DMPC based on a cooperative game does not and the MPC algorithm does not show a relevant improvement. It has been possible to verify that the improvement introduced by considering suspended solids in the MPC and DMPC algorithms is due more to the increase in the penalty for overflows and to the peculiar adaptive construction of fuzzy sets than to the optimization of the concentrations of suspended solids in the network.

Consequently, UDS control is fundamentally driven by level and flow dynamics, but the inclusion of the TSS concentration improves the industrial implementation of the controller.

Author Contributions: M.F. and P.V. conceived and defined the main approach; A.C. and M.F. performed the simulations; P.V. and M.F. took care of the simulation interpretations; writing—review and editing, M.F. and A.C. All authors have read and agreed to the published version of the manuscript.

Funding: This research was funded by Spanish Government through the MICINN projects PID2019-105434RB-C31 and TED2021-129201B-I00, and the Samuel Solórzano Foundation through project FS/11-2021.

Data Availability Statement: Not applicable.

Conflicts of Interest: The authors affirm that they have no conflict of interest.

Appendix A

Matrices of the model:

Appendix B

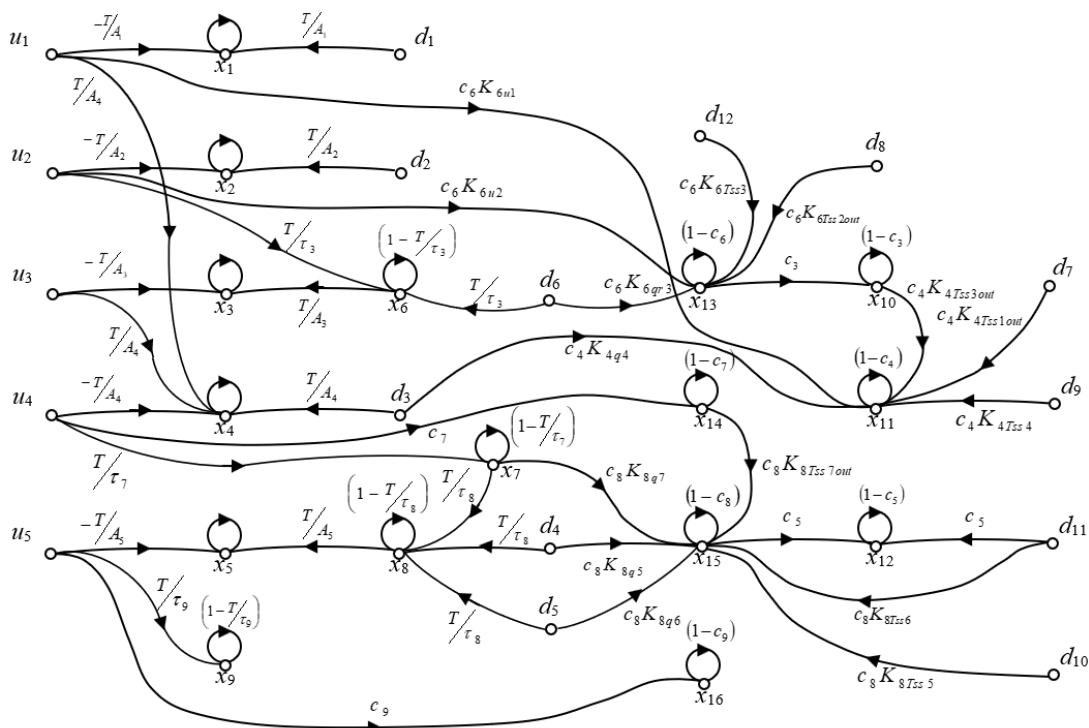


Figure A1. Direct graph of the model.

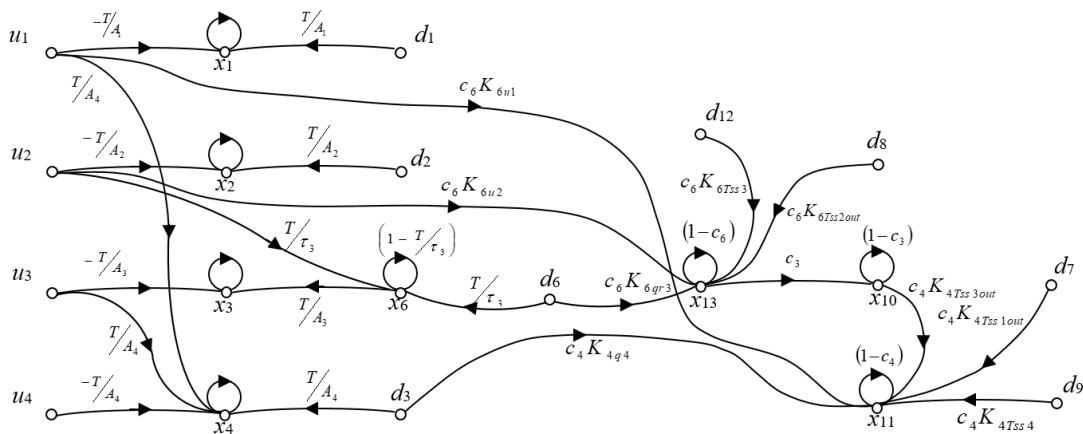


Figure A2. Subsystem 1.

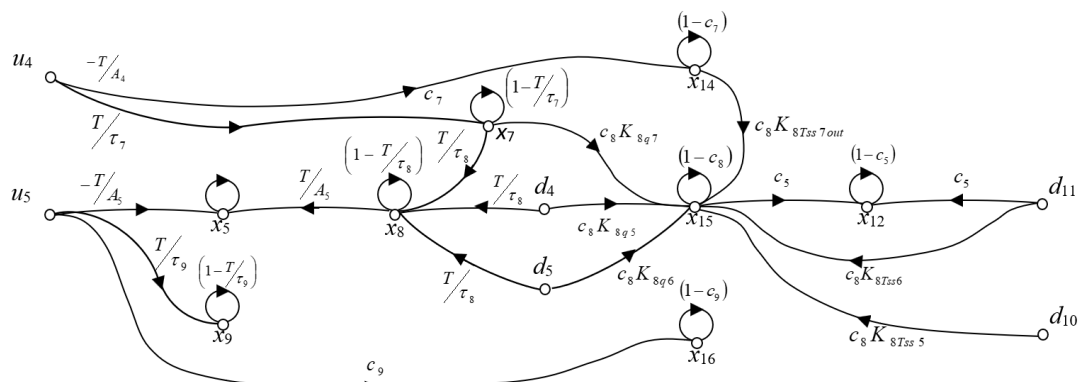


Figure A3. Subsystem 2.

References

1. Jamieson, D.G.; Shamir, U.; Martínez, F.; Franchini, M. Conceptual design of a generic, real-time, near-optimal control system for water-distribution networks. *J. Hydroinform.* **2007**, *9*, 3–14. [[CrossRef](#)]
2. Fu, G.; Khu, S.T.; Butler, D. Use of surrogate modelling for multiobjective optimisation of urban wastewater systems. *Water Sci. Technol.* **2009**, *60*, 1641–1647. [[CrossRef](#)] [[PubMed](#)]
3. Cho, J.H.; Sung, K.S.; Ha, S.R. A river water quality management model for optimizing regional wastewater treatment using a genetic algorithm. *J. Environ. Manag.* **2004**, *73*, 229–242. [[CrossRef](#)] [[PubMed](#)]
4. Fu, G.; Butler, D.; Khu, S.T. Multiple objective optimal control of integrated urban wastewater systems. *Environ. Model. Softw.* **2008**, *23*, 225–234. [[CrossRef](#)]
5. Saagi, R.; Flores-Alsina, X.; Fu, G.; Butler, D.; Gernaey, K.V.; Jeppsson, U. *Catchment & Sewer Network Simulation Model to Benchmark Control Strategies within Urban Wastewater Systems*; Elsevier: Amsterdam, The Netherlands, 2016.
6. Benedetti, L.; Langeveld, J.G.; Corneau, A.; Corominas, L.; Daigger, G.T.; Martin, C.; Mikkelsen, P.S.; Vezzaro, L.; Weijers, S.; Vanrolleghem, P.A. Modelling and monitoring of integrated urban wastewater systems: Review on status and perspectives. *Water Sci. Technol.* **2013**, *68*, 1203–1215. [[CrossRef](#)]
7. García, L.; Barreiro-Gómez, J.; Escobar, E.; Téllez, D.; Quijano, N.; Ocampo-Martínez, C. Modeling and Real-Time Control of Urban Drainage Systems: A review. *Adv. Water Resour.* **2015**, *85*, 120–132. [[CrossRef](#)]
8. Beenenken, T.; Erbe, V.; Messmer, A.; Reder, C.; Rohlfing, R.; Scheer, M.; Schuetze, M.; Schumacher, B.; Weilandt, M.; Weyand, M. Real time control (RTC) of urban drainage systems—A discussion of the additional efforts compared to conventionally operated systems. *Urban Water J.* **2013**, *10*, 293–299. [[CrossRef](#)]
9. Farina, M.; Scattolini, R. *Distributed MPC for Large-Scale Systems*; Springer: Berlin/Heidelberg, Germany, 2018.
10. Li, Z.; Duan, Z. *Cooperative Control of Multi-Agent Systems. A Consensus Region Approach*; CRC Press: Boca Raton, FL, USA, 2015.
11. Klepiszewski, K.; Schmitt, T. Comparison of conventional rule-based flow control with control processes based on fuzzylogic in a combined sewer system. *Water Sci. Technol.* **2002**, *46*, 77–84. [[CrossRef](#)]
12. Muschalla, D. Optimization of integrated urban wastewater systems using multi-objective evolution strategies. *Urban Water J.* **2008**, *5*, 57–65. [[CrossRef](#)]
13. Barbu, M.; Vilanova, R. Fuzzy Control Applied on a Benchmark Simulation Model for Sewer Networks. In Proceedings of the 20th International Conference on System Theory, Control and Computing (ICSTCC), Sinaia, Romania, 13–15 October 2016.

14. Regneri, M.; Klepiszewski, K.; Ostrowski, M.; Vanrolleghem, P.A. Fuzzy decision making for multicriteria optimization in integrated wastewater system management. In Proceedings of the 6th International Conference on Sewer Processes and Networks, Surfers Paradise, Australia, 7–10 November 2010; pp. 1–10.
15. Tagherouit, W.B.; Bennis, S.; Bengassem, J. A fuzzy expert system for prioritizing rehabilitation of sewer networks. *Comput. Aided Civ. Infrastruct. Eng.* **2011**, *26*, 146–152. [[CrossRef](#)]
16. Tang, W.; Wang, Z.; Feng, Q.; Wang, M. Application of fuzzy expert control to APMP pulping wastewater treatment process of aerobic. In Proceedings of the 2010 IEEE International Conference on Mechatronics and Automation, Xi'an, China, 4–7 August 2010; pp. 339–344. [[CrossRef](#)]
17. Marinaki, M.; Papageorgiou, M. Linear-quadratic regulators applied to sewer network flow control. In Proceedings of the European Control Conference, Cambridge, UK, 1–4 September 2003; pp. 1–4, ISBN 978-3-9524173-7-9.
18. Barreiro-Gómez, J.; Obando, G.; Riaño-Briceño, G.; Quijano, N.; Ocampo-Martínez, C. Decentralized control for urban drainage systems via population dynamics: Bogotá case study. In Proceedings of the European Control Conference, Linz, Austria, 15–17 July 2015.
19. Ramírez-Llanos, E.; Quijano, N. A population dynamics approach for the water distribution problem. *Int. J. Control.* **2010**, *83*, 1947–1964. [[CrossRef](#)]
20. Sun, C.; Bernat, J.D.; Cembrano, G.; Puig, V.; Meseguer, J. Advanced Integrated Real-Time Control of Combined Urban Drainage Systems using MPC. In Proceedings of the 13th International Conference on Hydroinformatics, Palermo, Italy, 1–6 July 2018.
21. Xu, M.; Van Overloop, J.; Van de Giesen, N.C. Model Reduction in Model Predictive Control of Combined Water Quantity and Quality in Open Channels. *J. Environ. Modell. Software* **2013**, *42*, 72–87. [[CrossRef](#)]
22. Vasiliev, I.; Luca, L.; Vilanova, R.; Caraman, S. Sewer Network Modelling and Control—A literature Review. In Proceedings of the 2022 26th International Conference on System Theory, Control and Computing (ICSTCC), Sinaia, Romania, 19–21 October 2022; ISBN 978-1-6654-6746-9. [[CrossRef](#)]
23. Schütze, M.; Campisano, A.; Colas, H.; Vanrolleghem, P.; Schilling, W. Real-time control of urban water systems. In Proceedings of the International Conference on Pumps, Electromechanical Devices and Systems Applied to Urban Water Management, Valencia, Spain, 22–25 April 2003; pp. 1–19.
24. Ocampo-Martínez, C.; Puig, V. *Modelling Approaches for Predictive Control of Large-Scale Sewage Systems*; Institut de Robòtica I Informàtica Industrial (IRI): Barcelona, Spain, 2009.
25. Ocampo-Martínez, C.; Puig, V.; Cembrano, G.; Quevedo, J. Application of predictive control strategies to the management of complex networks in the urban water cycle. *IEEE Control Syst. Mag.* **2013**, *33*, 15–41. [[CrossRef](#)]
26. Bach, P.M.; Rauch, W.; Mikkelsen, P.S.; McCarthy, D.T.; Deletic, A. A critical review of integrated urban water modelling—Urban drainage and beyond. *Environ. Model. Softw.* **2014**, *54*, 88–107. [[CrossRef](#)]
27. Keupers, I.; Willems, P. Development and Testing of a Fast Conceptual River Water Quality Model. *Water Res.* **2017**, *113*, 62–71. [[CrossRef](#)]
28. Rauch, W.; Bertrand-Krajewski, J.L.; Krebs, P.; Mark, O.; Schilling, W.; Schütze, M.; Vanrolleghem, P.A. Deterministic modelling of integrated urban drainage systems. *Water Sci. Technol.* **2002**, *45*, 81–94. [[CrossRef](#)]
29. Kroll, S.; Fenu, A.; Wambecq, T.; Weemaes, M.; Van Impe, J.; Willems, P. Energy Optimization of the Urban Drainage System by Integrated Real-Time Control during Wet and Dry Weather Conditions. *Urban Water J.* **2018**, *15*, 362–370. [[CrossRef](#)]
30. Meneses, E.J.; Gaussens, M.; Jakobsen, C.; Mikkelsen, P.S.; Grum, M.; Vezzaro, L. Coordinating Rule-Based and System-Wide Model Predictive Control Strategies to Reduce Storage Expansion of Combined Urban Drainage Systems: The Case Study of Lundtofte, Denmark. *Water* **2018**, *10*, 76. [[CrossRef](#)]
31. Maciejowski, J.M. *Predictive Control with Constraints*; Pearson Education Limited, Prentice-Hall: London, UK, 2002.
32. Qin, S.J.; Badgwell, T.A. A survey of industrial model predictive control technology. *Control Eng. Pract.* **2003**, *11*, 733–764. [[CrossRef](#)]
33. Rawlings, J.; Mayne, D. *Model Predictive Control: Theory and Design*; Nob Hill Publishing: Madison, WI, USA, 2017.
34. Cembrano, G.; Quevedo, J.; Salamero, M.; Puig, V.; Figueras, J.; Martí, J. Optimal control of urban drainage systems, a case study. *Control Eng. Pract.* **2004**, *12*, 1–9. [[CrossRef](#)]
35. Ocampo-Martínez, C. *Model Predictive Control of Wastewater Systems*; Springer: London, UK, 2011. [[CrossRef](#)]
36. Giraldo, J.; Leirens, S.; Díaz-Granados, M.; Rodríguez, J. Nonlinear optimization for improving the operation of sewer systems: The Bogotá case study. In Proceedings of the International Congress on Environmental Modelling and Software Modelling for Environments Sake, Ottawa, ON, Canada, 5–8 July 2010; pp. 1–8.
37. Sun, C.; Joseph-Duran, B.; Maruejouls, T.; Cembrano, G.; Meseguer, J.; Puig, V.; Lítrico, X. Real-Time Control-Oriented Quality Modelling in Combined Urban Drainage Networks. *IFAC Pap.* **2017**, *50*, 3941–3946. [[CrossRef](#)]
38. Svensen, J.L.; Niemann, H.H.; Poulsen, N.K. Model Predictive Control of Overflow in Sewer Networks: A comparison of two methods. In Proceedings of the 2019 4th Conference of Control and Fault Tolerant Systems (SysTol), Casablanca, Morocco, 18–20 September 2019; pp. 412–417. [[CrossRef](#)]
39. Barcelli, D. Optimal Decomposition of Barcelona's Water Distribution Network System for Applying Distributed Model Predictive Control. Master's Thesis, Universitat Politècnica de Cataluña-IRI-Università degli Studi di Siena, Barcelona, Spain, 2008.
40. Real, A.J.D.; Arce, A.; Bordons, C. Combined environmental and economic dispatch of smart grids using distributed model predictive control. *Electr. Power Energy Syst.* **2014**, *54*, 65–76. [[CrossRef](#)]

41. Leirens, S.; Zamora, C.; Negenborn, R.R.; De Schutter, B. Coordination in urban water supply networks using distributed model predictive control. In Proceedings of the 2010 American Control Conference, Baltimore, MD, USA, 30 June–2 July 2010; pp. 3957–3962. [[CrossRef](#)]
42. Francisco, M.; Mezquita, Y.; Revollar, S.; Vega, P.; De Paz, J.F. Multi-agent distributed model predictive control with fuzzy negotiation. *Expert Syst. Appl.* **2019**, *129*, 68–83. [[CrossRef](#)]
43. Masero, E.; Francisco, M.; Maestre, J.M.; Revollar, S.; Vega, P. Hierarchical distributed model predictive control based on fuzzy negotiation. *Expert Syst. Appl.* **2021**, *176*, 114836. [[CrossRef](#)]
44. Ocampo-Martínez, C.; Puig, V.; Grosso, J.; de Oca, S.M. Multi-layer decentralized MPC of large-scale networked systems. In *Distributed Model Predictive Control Made Easy*; Springer: Berlin/Heidelberg, Germany, 2014; pp. 495–515. [[CrossRef](#)]
45. Maestre, J.M.; Muñoz De La Peña, D.; Camacho, E.F. Distributed model predictive control based on a cooperative game. *Optim. Control Appl. Methods* **2011**, *32*, 153–176. [[CrossRef](#)]
46. Cembellín, A.; Francisco, M.; Vega, P. Distributed Model Predictive Control Applied to a Sewer System. *Processes* **2020**, *8*, 64. [[CrossRef](#)]
47. Siljak, D.D. *Decentralized Control of Complex Systems*; Dover Publications, Inc.: Mineola, NY, USA, 1991.
48. Kroll, S.; Weemaes, M.; Van Impe, J.; Willems, P. A Methodology for the Design of RTC Strategies for Combined Sewer Networks. *Water* **2018**, *10*, 1675. [[CrossRef](#)]
49. Marinaki, M. *Optimal Real-Time Control of Sewer Networks*; Springer: Berlin/Heidelberg, Germany, 2005.
50. Alex, J.; Schütze, M.; Ogurek, M.; Jumar, U. Systematic Design of Distributed Controllers for Sewer Networks. In Proceedings of the 17th World Congress IFAC, Seoul, Republic of Korea, 6–11 July 2008.
51. Mayne, D.Q.; Rawlings, J.B.; Rao, C.V.; Scokaert, P.O.M. *Constrained Model Predictive Control: Stability and Optimality*; Elsevier: Amsterdam, The Netherlands, 2000.
52. Maestre, J.M.; Muñoz de la Peña, D.; Camacho, E.F.; Álamo, T. Distributed model predictive control based on agent negotiation. *J. Process Control* **2011**, *21*, 685–697. [[CrossRef](#)]
53. Yager, R.; Filev, D. *Essentials of Fuzzy: Modeling and Control*; Wiley Interscience: New York, NY, USA, 1994.
54. Zadeh, L.A.; Aliev, R.A. *Fuzzy Logic Theory and Applications: Part I and Part II*; World Scientific: Hackensack, NJ, USA, 2018.

Disclaimer/Publisher's Note: The statements, opinions and data contained in all publications are solely those of the individual author(s) and contributor(s) and not of MDPI and/or the editor(s). MDPI and/or the editor(s) disclaim responsibility for any injury to people or property resulting from any ideas, methods, instructions or products referred to in the content.